Chemical Engineering Journal 153 (2009) 9–15

Contents lists available at ScienceDirect

Chemical Engineering Journal

journal homepage: www.elsevier.com/locate/cej

Photoassisted hetero-Fenton mineralisation of azo dyes by Fe(II)-Al_2O_3 catalyst

B. Muthukumari, K. Selvam, I. Muthuvel, M. Swaminathan*

Department of Chemistry, Annamalai University, Annamalainagar 608 002, Tamilnadu, India

ARTICLE INFO

Article history:
Received 23 November 2007
Received in revised form 12 May 2009
Accepted 17 May 2009

Keywords:
Heterogeneous photo-Fenton
Direct Red 23
Reactive Orange 4
Ferrous sulfate
Al_2O_3

ABSTRACT

Photoassisted Fenton mineralisation of two azo dyes Direct Red 23 (DR 23) and Reactive Orange 4 (RO 4) was studied in detail using a Fe(II) loaded Al_2O_3 as a heterogeneous catalyst in presence of H_2O_2 and UV-A light. 25 and 15% $FeSO_4$ loaded Al_2O_3 show the maximum efficiency in the degradation of DR 23 and RO 4 respectively. The effects of catalyst loading, H_2O_2 concentration, initial solution pH and initial dye concentration on photodegradation were investigated and the optimum conditions are reported. DR 23 undergoes easy degradation when compared to RO 4. The difference is due to the presence of stable triazine ring system in RO 4. The catalyst is reusable and the leaching of Fe(II) from the catalyst in each run is less than 10% in the pH range 2–7.

1. Introduction

Though Fenton reactions were known for more than a century [1], it was reported as a method for wastewater treatment since 1990s [2–5]. The photochemically enhanced Fenton reactions are considered most promising for the remediation of wastewater containing a variety of toxic chemicals [6–10]. The higher efficiency of photo-Fenton reaction is due to the efficient recycling of Fe^{2+} than the thermal process [11]. Among the advanced oxidation processes, photo-Fenton process was reported to be more efficient and economical [12]. However, the use of Fe(II)/Fe(III) as a homogeneous catalyst has a significant disadvantage. The removal of sludge containing Fe ions at the end of wastewater treatment is costly and needs large amount of chemicals and manpower. In this context the photocatalytic degradation of organic contaminants using heterogeneous photo-Fenton catalyst will be more preferred. A number of heterogeneous catalysts developed by immobilizing Fe(II)/Fe(III) ions on various supports had been reported in the literature [13–18].

Earlier we had investigated the photodegradation of various dyes using some modified semiconductor [19,20] and Fenton [14,21] photocatalysts. In this paper, we report the preparation and charecterisation of Fe(II) loaded Al_2O_3 as heterogeneous catalyst and the photodegradation of two azo dyes, namely DR 23, RO 4 with this catalyst using UV light.

2. Experimental

2.1. Chemicals

The commercial azo dyes Direct Red 23, Reactive Orange 4 (Colour Chem, Pondicherry), AnalaR H_2O_2 (30%, w/w), $FeSO_4{\cdot}7H_2O$ (Merck), neutral Al_2O_3 with the particle size 70–280 mesh (Loba Chemicals), H_2SO_4, NaOH (Qualigens) were used as received. The experimental solutions were prepared using distilled water. The dye structures with their absorption maxima are given in Fig. 1.

2.2. Preparation of catalyst

Five gram of Al_2O_3 and required percentage (15, 25, 35 and 45%) of ferrous sulfate were added to ethanol/water mixture (60:40). The suspension was stirred for 3–4 h. Then the pale yellowish coloured Fe^{2+} loaded Al_2O_3 catalyst was filtered and dried. These Fe^{2+} loaded Al_2O_3 catalysts obtained by the addition of different concentration of Fe_2SO_4 were tested for their degradation efficiencies under the same conditions.

2.3. Apparatus

The specific surface area of the catalyst was determined through nitrogen adsorption at 77 K on the basis of BET equation using a Sorptomatic 1990 instrument. Scanning electron microscopic (SEM) analysis was performed on platinum coated samples using a

* Corresponding author. Tel.: +91 4144 220572; fax: +91 4144 220572.
E-mail address: chemres50@gmail.com (M. Swaminathan).

1385-8947/$ – see front matter © 2009 Elsevier B.V. All rights reserved.
doi:10.1016/j.cej.2009.05.030

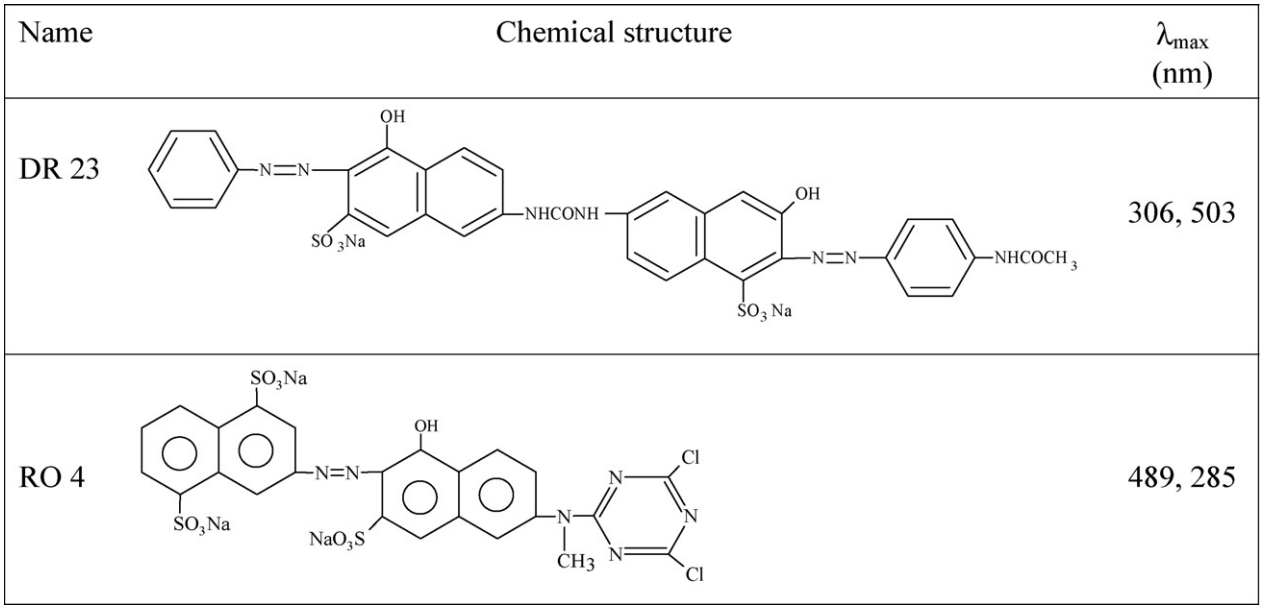

Fig. 1. Structures of DR 23 and RO 4.

JEOL apparatus model JSM-5610 LV, equipped with an INCA EDX probe for the energy dispersive X-ray micro-analysis (EDX). UV spectral measurements were made using Hitachi U-2001 spectrophotometer. The pH of the solution was measured using HANNA Phep (Model H 198107) digital pH meter. The amount of ferrous ion present in the catalyst and amount of ferrous ion leached from the catalyst in each run was determined using ELICO SL-176 model Atomic Absorption Spectrometer.

Heber multilamp photoreactor model HML-MP 88 was used for photoreaction. This model consists of eight medium pressure mercury vapor lamps of 8 W set in parallel emitting 365 nm wavelength. It has a reaction chamber with specially designed reflectors made of highly polished aluminium and built in cooling fan at the bottom. It is provided with the magnetic stirrer at the centre. Open borosilicate glass tube of 50 mL capacity, 40 cm height and 12.6 mm diameter was used as a reaction vessel with the total radiation exposure length of 330 mm. The irradiation was carried out using four parallel medium pressure mercury lamps (32 W) in open-air condition. The light intensity was measured by ferrioxalate actinometry [22] and it is found to be 1.381×10^{-6} einstein L^{-1} s^{-1}. The solution with Fe^{2+}-Al_2O_3 with H_2O_2 and dye was continuously aerated by a pump to provide oxygen and for complete mixing of reaction medium.

2.4. Procedure

In all experiments 50 mL of reaction mixture was irradiated. At specific time intervals 1 mL of the sample was withdrawn and centrifuged to separate the Fe^{2+}-Al_2O_3 catalyst. NaOH solution was used to quench the oxidation by raising the pH to 10. At this pH further generation of hydroxyl radical is prevented. 1 mL of the sample was suitably diluted and its absorbances at 306 and 503 nm for DR 23 or at 285 and 489 nm for RO 4 were measured immediately. The absorbances at 306 and 285 nm for DR 23 and RO 4 ($\pi \rightarrow \pi^*$ transition in naphthalene group) represent the aromatic content of the dyes and the decrease at these wavelengths for various time intervals indicates the degradation of aromatic part of dyes. The evolution CO_2 was tested by the formation of $CaCO_3$ when the gas evolved during the reaction was passed into lime-water.

3. Results and discussion

3.1. Characterization of catalyst

The catalyst prepared with 25% $FeSO_4$ loading was characterized. BET surface area of Fe(II)-Al_2O_3 (25%) catalyst is 77 m^2 g^{-1}. Both Fe^{2+} loaded and bare catalyst have the particle 10 μm in size. Fig. 2 shows the SEM images of Al_2O_3 and Fe(II)-Al_2O_3 (25%). Iron crystallites are covered throughout the Al_2O_3 matrix (Fig. 2b). The EDX diagram of the catalyst (Fig. 3) reveals the percentages of iron and aluminium at one region. The FT-IR spectra of pure Al_2O_3 and Fe(II)-Al_2O_3 (25%) are shown in Fig. 4a and b. The major peaks appearing in the FT-IR spectra may be related to the following: (i) –OH stretching vibrations of the surface bonded (or) adsorbed water, (ii) –OH stretching vibrations of structural water corresponding to M-OH stretching, (iii) –OH bending vibrations of structural water, corresponding to M-OH bending and (iv) Al–O and Fe–O vibrations [23]. The peaks 3451 and 3426 cm^{-1} observed in Fig. 4a and b account for surface bonded –OH stretching in Al_2O_3. A small broad peak at 1634 cm^{-1} corresponds to bending vibrations –OH in pure Al_2O_3. This peak is narrowed down at 1644 cm^{-1} in Fe(II)-Al_2O_3 (25%). This and other frequencies at 1401 cm^{-1} are due to the bending vibrations of OH bound with Fe^{2+} present on the surface of Al_2O_3. The results reveal the presence of Fe ion on the surface of Al_2O_3.

3.2. Primary analysis of DR 23 and RO 4

The photocatalytic activity of the Fe(II)-Al_2O_3 (25%) was evaluated by the degradation of two different azo dyes, namely DR 23, RO 4. Controlled experiments under different reaction conditions were carried out for both dyes and the results are displayed in Figs. 5 and 6 for DR 23 and RO 4 respectively. It is clear that both dyes are resistant to direct photolysis by UV-A light (Figs. 5 and 6, curve a). There is no decrease in the concentration of dyes when they are treated with Fe^{2+}-Al_2O_3 (25%)/dark.

Irradiation of DR 23 in the presence of ferrous ion alone gives about 10% removal (Fig. 5, curve b). In the presence of H_2O_2 and UV light decrease of dye occurs continuously (curve c). For Fe^{2+}/H_2O_2/dark (curve d), 22.5% of degradation in DR 23 was observed at the time of 20 min irradiation. A higher dye removal

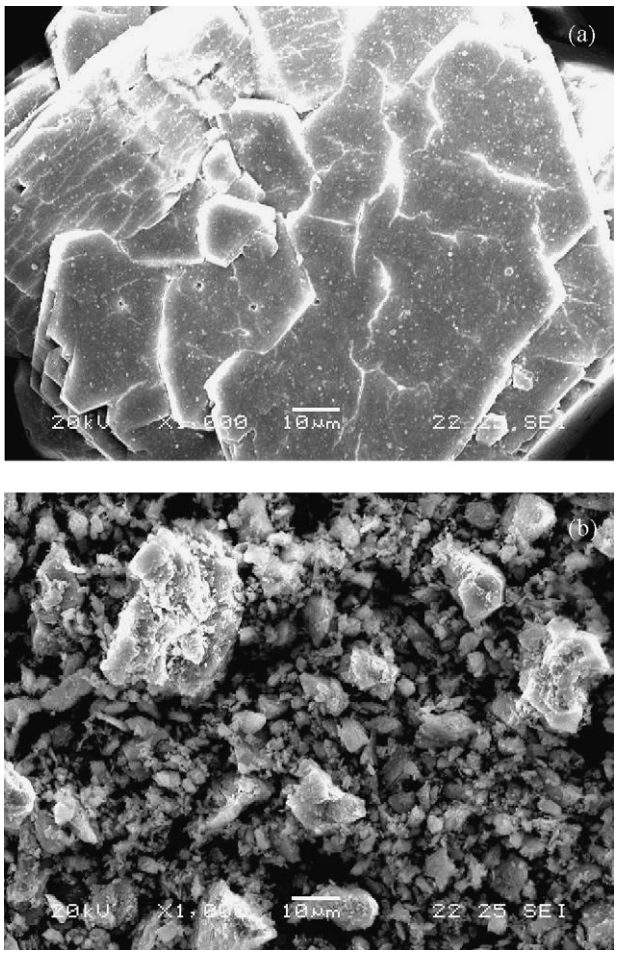

Fig. 2. Scanning electron microscope images: (a) Al_2O_3 and (b) Fe^{2+} (25%)/Al_2O_3.

in Fe^{2+}/H_2O_2/dark when compared to UV/H_2O_2 shows that the Fe^{2+} catalyzed decomposition of H_2O_2 is more than the UV catalyzed decomposition of H_2O_2. The quantum yield of formation of •OH in UV/H_2O_2 is also dependent on the wavelength and intensity of light. The quantum yield of formation of hydroxyl radical at 365 nm is low and hence low removal rate is observed. The trend observed is the same under the above conditions for RO 4 (Fig. 6, curves b–d).

The dyes DR 23 and RO 4 on irradiation with heterophoto-Fenton catalyst Fe(II)-Al_2O_3 (25%)/H_2O_2 undergo 100 and 75% degradations in 60 min respectively (Figs. 5 and 6, curve f). In order to compare the heterogeneous photo-Fenton reaction with that of homogeneous system, we have taken same amount of Fe^{2+} present in heterophoto-Fenton catalyst. Initially up to 40 min the homogeneous photo-Fenton process is fast (Figs. 5 and 6, curve e). The percentages of degradation for both homogeneous and heterogeneous processes at 60 min are almost same. But the heterogeneous photo-Fenton catalyst has the advantages of easy removal and reusability. The effects of various parameters on photo-Fenton degradation of DR 23 and RO 4 with Fe^{2+}-Al_2O_3 catalyst have been investigated.

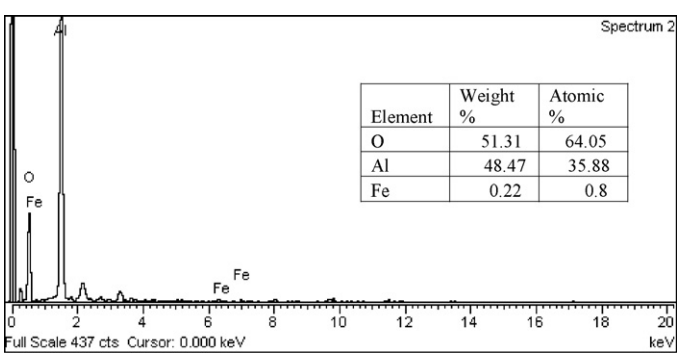

Fig. 3. EDX diagram for Fe^{2+} (25%)/Al_2O_3.

3.3. Effect of Fe^{2+} loading on Al_2O_3

The effect of iron loading of Al_2O_3 has been investigated employing different concentrations of ferrous sulfate by weight. The catalysts prepared with 15, 25, 35 and 45% ferrous sulfate were used for the degradation of both dyes. 50 mg of these catalysts was used for photodegradation of DR 23 and RO 4. The degradation follows

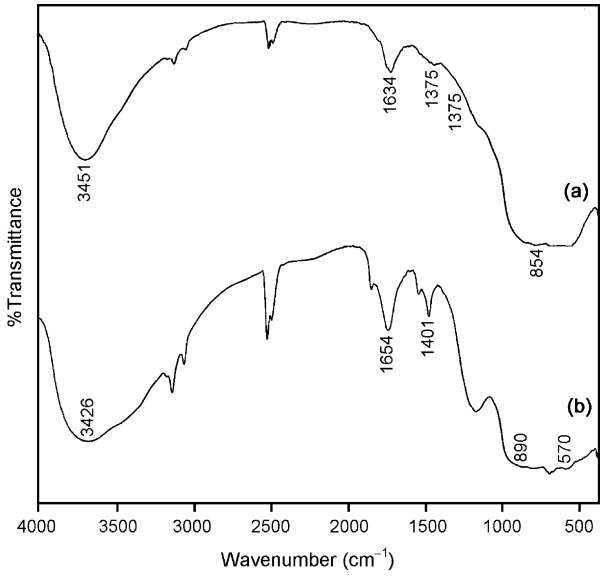

Fig. 4. FT-IR spectra of (a) Al_2O_3 and (b) Fe^{2+} (25%)/Al_2O_3.

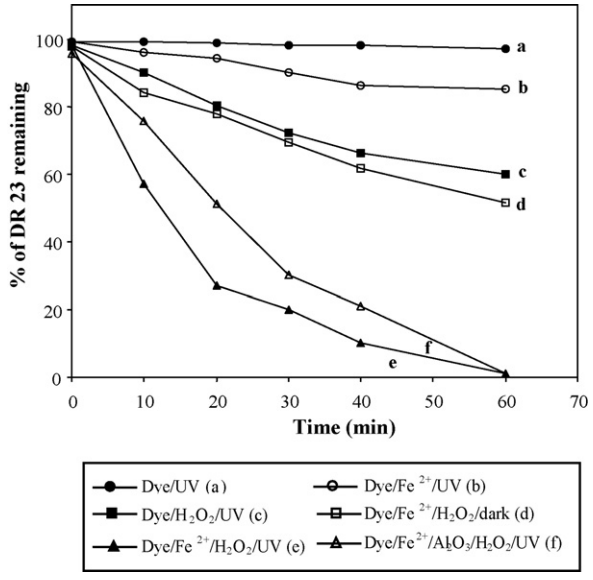

Fig. 5. Primary analysis of DR 23; [DR 23] = 5×10^{-4} M, Fe^{2+} (25%)/Al_2O_3 = 1 g L^{-1}, H_2O_2 = 10 mmol L^{-1}, pH = 3 ± 0.1, airflow rate = 8.1 mL s^{-1}, and $I_0 = 1.381 \times 10^{-6}$ einstein L^{-1} s^{-1}.

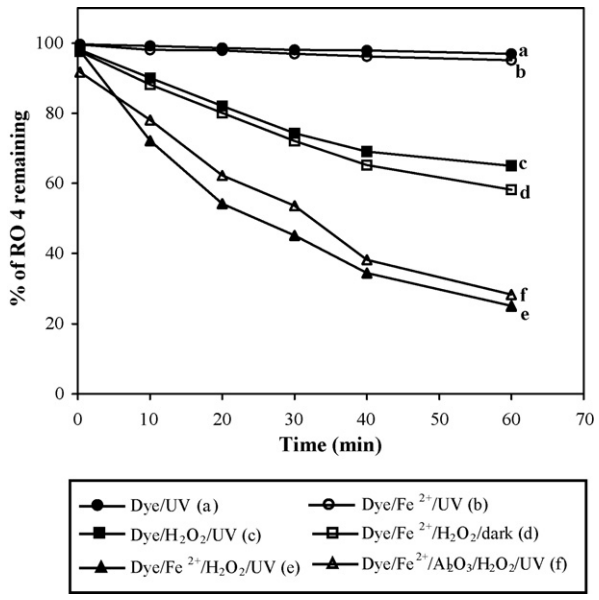

Fig. 6. Primary analysis of RO 4; [RO 4] = 5×10^{-4} M, Fe^{2+} (25%)/Al_2O_3 = 1 g L^{-1}, H_2O_2 = 10 mmol L^{-1}, pH = 3 ± 0.1, $I_0 = 1.381 \times 10^{-6}$ einstein L^{-1} s^{-1}, and airflow rate = 8.1 mL s^{-1}.

the *pseudo*-first order kinetics (Eq. (1)):

$$\ln\left(\frac{C_0}{C}\right) = kt \quad (1)$$

where k is the *pseudo*-first order rate constant, C_0 is the initial concentration of dye and C is the concentration at time 't'. The rate constants were determined from the slope of the linear plots of $\ln(C_0/C)$ vs. t. The variation of rate constants for the catalysts prepared with different ferrous sulfate concentrations for the dyes DR 23 and RO 4 are shown in Fig. 7a and b.

The DR 23 removal increases with increase in $FeSO_4$ loading from 15 to 25% and then decreases. For 25% $FeSO_4$ loading the rate constants for decolourisation and degradation are 0.03 and 0.02 min^{-1} respectively. In the case of RO 4, the dye removal increases with increase in $FeSO_4$ loading from 10 to 15% and then decreases. For 15% $FeSO_4$ loading the rate constants of decolourisation and degradation are 0.086 and 0.030 min^{-1} respectively. Hence under these experimental conditions 25 and 15% of $FeSO_4$ were found to be optimum for efficient removal of DR 23 and RO 4 respectively.

3.4. Effect of pH

The effect of initial pH on the Fe^{2+}-Al_2O_3 degradation rate of DR 23 and RO 4 was investigated and the results are shown in Fig. 8a and b. In DR 23, increase of pH from 1 to 2 increases the pseudo-first order rate constant from 0.011 to 0.053 min^{-1} for degradation. Further increase of pH above 2 decreases the rate constant. Hence pH 2 is optimum for heterogeneous photo-Fenton degradation of DR 23. In the case of RO 4, increase of pH from 1 to 3 increases the pseudo-first order rate constant for degradation from 0.008 to 0.031 min^{-1}. Further increase of pH above 3 decreases the rate constant. The maximum degradation of RO 4 is observed within 60 min at pH 3. Hence in both dyes the maximum degradation efficiency was observed at acidic pH similar to homogeneous Fenton process. This indicates that the mechanism of degradation is same for both heterogeneous and homogeneous degradations.

To find out the reason for the difference in efficiencies at different pH, the experiment on adsorption of dye on the catalyst at various pH was carried out for both dyes. The percentages of adsorption of DR 23 on the catalyst are found to be 36, 48, 61, 57 and 4 at pH 1, 2, 3, 4 and 6 respectively. In case RO 4, the percentages of dye adsorption are 2,7,25, 22, and 12, at 1, 2, 3, 4, and 6 respectively. The adsorption of DR 23 is more than that of RO 4. Since the adsorption of dye is maximum at pH 3, more degradation occurs at this pH.

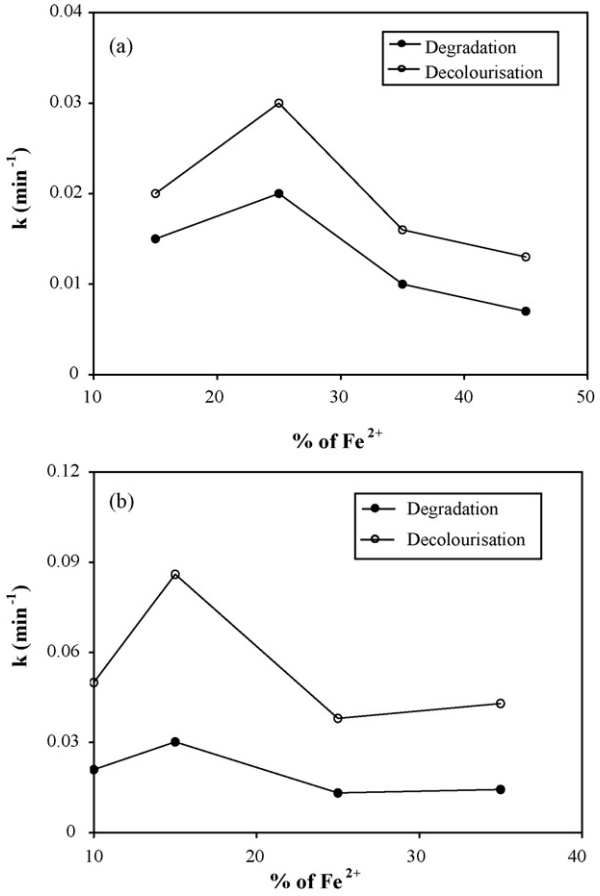

Fig. 7. Effect of Fe^{2+} loading on Al_2O_3 for dye removal: dye = 5×10^{-4} M, catalyst suspended = 1 g L^{-1}, H_2O_2 = 10 mmol L^{-1}, airflow rate = 8.1 mL s^{-1}, pH = 3 ± 0.1, $I_0 = 1.381 \times 10^{-6}$ einstein L^{-1} s^{-1}, (a) DR 23 and (b) RO 4.

3.5. Effect of H_2O_2 dosage

The degradation of DR 23 and RO 4 with Fe(II)-Al_2O_3 at different H_2O_2 concentrations was studied. Addition of H_2O_2 from 5 to 10 mmol L^{-1} increases the *pseudo*-first order rate constants for the degradation (0.015 to 0.025 min^{-1}) and decolourisation of DR 23 (0.022 to 0.033 min^{-1}) (Fig. 9a). Further increase of H_2O_2 above 10 mmol L^{-1} decreases the DR 23 degradation and decolourisation.

In the case of RO 4, addition of H_2O_2 from 5 to 15 mmol L^{-1} increases the pseudo-first order rate constants for degradation from 0.025 to 0.031 min^{-1} and the rate constant value for decolourisation increases from 0.083 to 0.1262 min^{-1} at the time of 40 min (Fig. 9b). Further increase of H_2O_2 above 15 mmol L^{-1} decreases the RO 4 degradation and decolourisation. Hence 10 and 15 mmol L^{-1} of H_2O_2 are the optimum concentrations for the degradation and decolourisation of DR 23 and RO 4 respectively. The increase in degradation efficiency is due to increased production of •OH radicals.

At H_2O_2 dosage above optimum level the decrease in removal rate is due to hydroxyl radical scavenging effect of H_2O_2 (Eqs. (2) and (3)) [13]:

$$H_2O_2 + {}^{\bullet}OH \rightarrow HO_2{}^{\bullet} + H_2O \quad (2)$$

$$HO_2{}^{\bullet} + {}^{\bullet}OH \rightarrow H_2O + O_2 \quad (3)$$

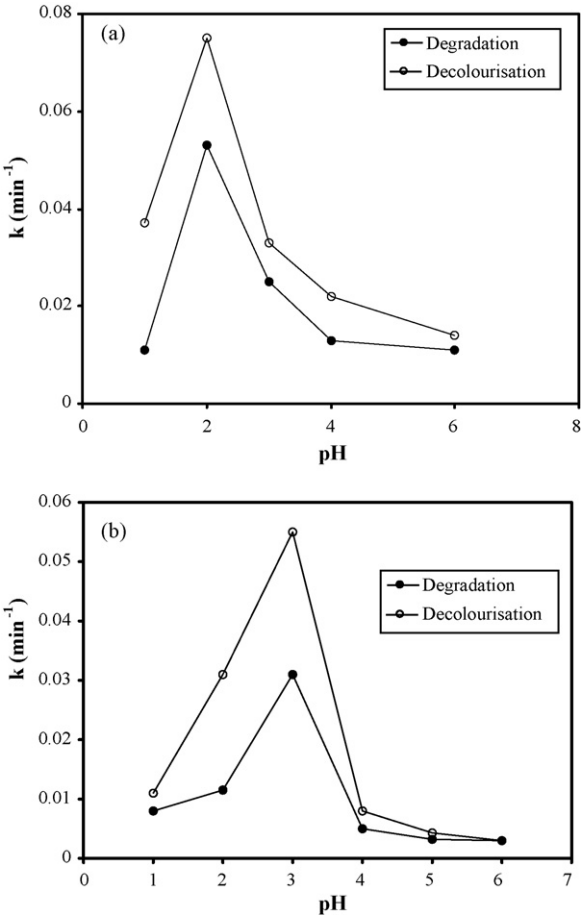

Fig. 8. Effect of solution pH for dye removal: dye = 5×10^{-4} M, catalyst suspended = 1 g L^{-1}, H_2O_2 = 10 mmol L^{-1}, airflow rate = 8.1 mL s^{-1}, $I_0 = 1.381 \times 10^{-6}$ einstein L^{-1} s^{-1}, (a) DR 23 and (b) RO 4.

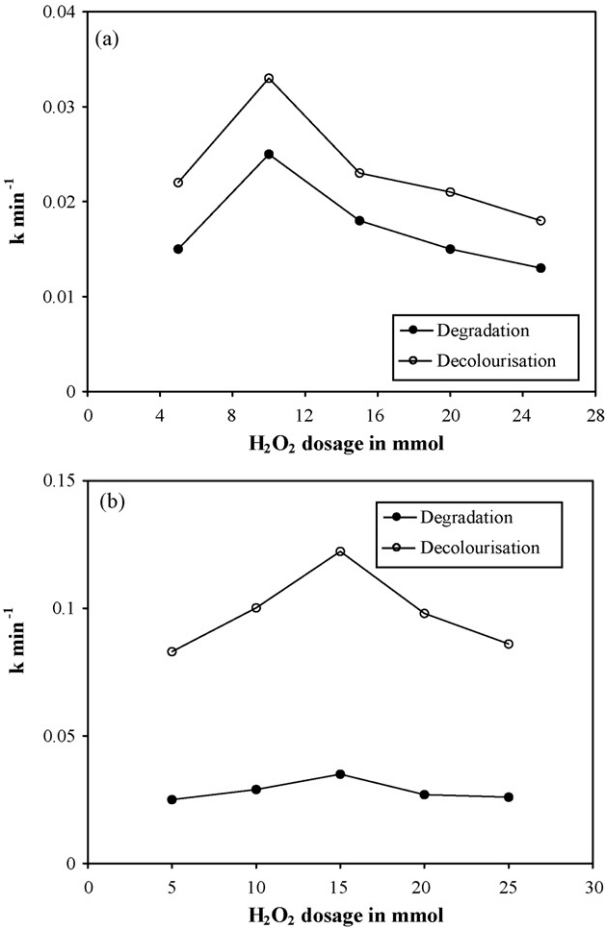

Fig. 9. Effect of H_2O_2 dosage for dye removal: dye = 5×10^{-4} M, catalyst suspended = 1 g L^{-1}, airflow rate = 8.1 mL s^{-1}, pH = 2 ± 0.1, $I_0 = 1.381 \times 10^{-6}$ einstein L^{-1} s^{-1}, (a) DR 23 and (b) RO 4.

3.6. Effect of initial dye concentration

Many researchers have investigated the effect of initial concentration on the degradation of dyes in solution. Increase of the initial concentration of both dyes from 3 to 6×10^{-4} M decreases the degradation from 0.055 to 0.018 min^{-1} in DR 23 and 0.0609 to 0.01509 min^{-1} in RO 4 at the time of 40 min (Fig. 10a and b). At high dye concentrations dye molecules may absorb a significant amount of 365 nm light and this reduces the absorbance of light by the catalyst. The increase in dye concentration also decreases the path length of photon entering this solution. It should be pointed out that even at a high initial concentrations of DR 23 and RO 4 (6×10^{-4} M) about 65 and 58% removal could be achieved respectively in 40 min. This indicates that Fe(II)-Al_2O_3 catalyst can also work well at high initial concentrations of dyes.

3.7. Effect of UV light intensity

The effect of UV power on decolourisation and degradation of DR 23 and RO 4 is shown in Fig. 11a and b. The light intensity was varied using 2, 4, 6, 8 lamps of 8 W each. Increase of UV power from 16 to 64 W increases the decolourisation and degradation in Fe(II)-Al_2O_3 processes. The UV power is mainly used for (i) photolysis of H_2O_2 (Eq. (4)), (ii) photoreduction of ferric to ferrous ions. Since all these processes are strongly dependent on wavelength and light intensity, photodegradation increases with increase in UV power. It is found that the UV power tested in our study lies in the linear range and all photons produced are effectively used:

$$H_2O_2 + h\nu \rightarrow {}^{\bullet}OH + OH^- \quad (4)$$

3.8. Long-term stability

The stability and reusability of the heterogeneous photo-Fenton catalyst were tested for DR 23 removal and the results are shown in Fig. 12. About 92% DR 23 removal takes place at 60 min in the first run. The same catalyst was separated, dried and used again. In the second run 53% of dye was removed at 60 min. Third run gave 42% dye removal. The initial decrease in efficiency in second run is high (39%) but the decrease in the third run is only 11%. The decrease in efficiency may be due to leaching of Fe^{2+} in each run. Amount of Fe^{2+} leached for the degradation of DR 23 in each run at different pH was measured using Atomic absorption spectrometer and the results are presented in Table 1. Amount of total Fe^{2+} in

Table 1
Amount of Fe^{2+} ion leached for the degradation of DR 23 in each run at different pH.

Run	pH 2	pH 5	pH 7
I	0.49 (7.3%)	0.33 (4.93%)	0.29 (4.33%)
II	0.45 (6.72%)	0.32 (4.78%)	0.26 (3.88%)
III	0.43 (6.42%)	0.30 (4.48%)	0.26 (3.88%)

Catalyst suspended = 1 g L^{-1}, irradiation time = 60 min airflow rate = 8.1 mL s^{-1}, $I_0 = 1.381 \times 10^{-6}$ einstein L^{-1} s^{-1}, DR 23 concentration = 5×10^{-4} M, Fe^{2+} = 15%, and H_2O_2 = 10 mmol L^{-1}.

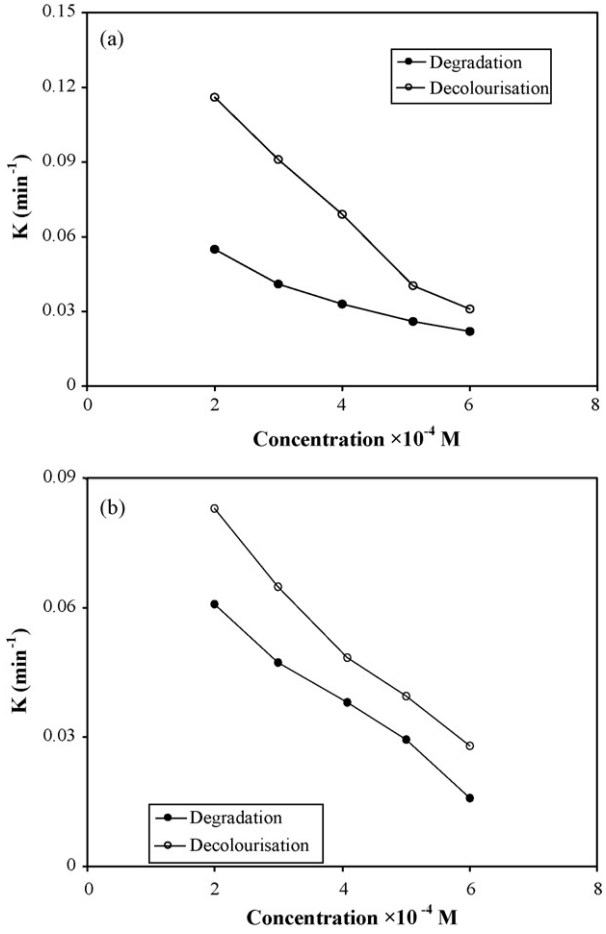

Fig. 10. Effect of initial dye concentration on the dye removal: catalyst suspended = 1 g L^{-1}, airflow rate = 8.1 mL s^{-1}, (a) DR 23: pH = 2 ± 0.1, Fe^{2+} = 25%, H_2O_2 = 10 mmol L^{-1}, and $I_0 = 1.381 \times 10^{-6}$ einstein L^{-1} s^{-1}; (b) RO 4: pH = 3 ± 0.1, Fe^{2+} = 15%, H_2O_2 = 15 mmol L^{-1}, and $I_0 = 1.381 \times 10^{-6}$ einstein L^{-1} s^{-1}.

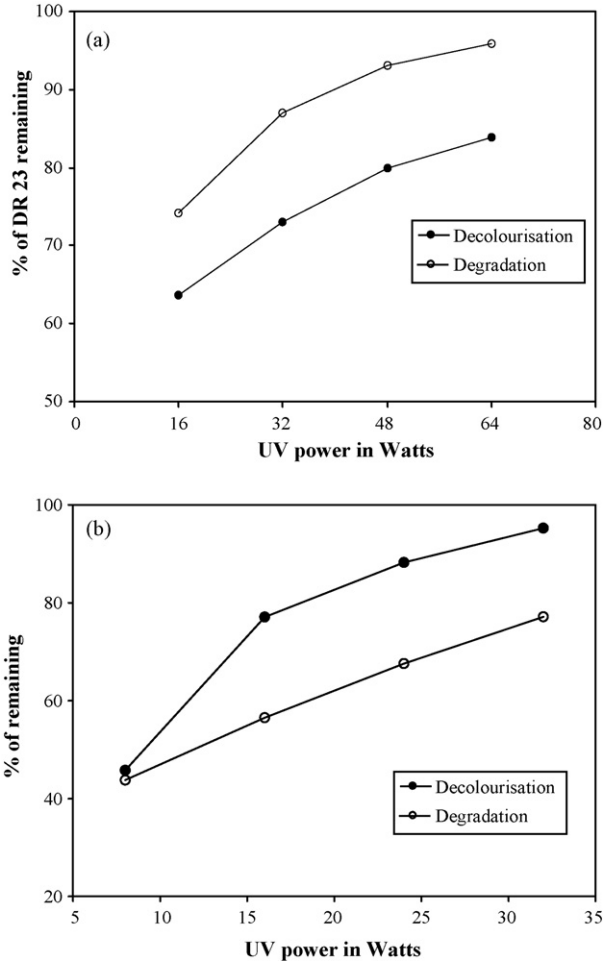

Fig. 11. Effect of light intensity on the dye removal: catalyst suspended = 1 g L^{-1}, airflow rate = 8.1 mL s^{-1}, $I_0 = 1.381 \times 10^{-6}$ einstein L^{-1} s^{-1}. (a) DR 23; pH = 2 ± 0.1, Fe^{2+} = 25%, and H_2O_2 = 10 mmol L^{-1}; (b) RO 4, pH = 3 ± 0.1, Fe^{2+} = 15%, and H_2O_2 = 15 mmol L^{-1}.

Fe(II)-Al_2O_3 (25% ferrous sulfate loaded) was found to be 6.69 ppm. The percentage of Fe ion leached from the catalyst was around 7% at pH 2 and it was less than 5% at pH 5 and 7 in each run. The leaching is slightly higher at acidic condition (pH 2) and it is minimum at pH 5 and 7. The Fe ion leaching decreases in each run and after the third run the leaching is not significant. Fe ion leaching decreases with increase in pH. Since the trend observed in leaching is the same as in catalytic efficiency, the decrease in efficiency for three runs is due to leaching. As there is no leaching and change in efficiency after third run, the catalyst is reusable.

3.8.1. Dye degradation mechanism

Based on the above results the following mechanism is proposed for heterogeneous photo-Fenton degradation of dyes using Fe^{2+}-Al_2O_3:

$$Fe^{2+}\text{on the non-reactive surface of } Al_2O_3 + H_2O_2 \rightarrow Fe^{3+}\text{on the non-reactive surface of } Al_2O_3 + {}^{\bullet}OH\,(\text{solution}) + {}^{-}OH$$

$$\text{dye} + {}^{\bullet}OH\,(\text{solution}) \rightarrow \text{reaction intermediates} \rightarrow CO_2 + H_2O + \text{mineral acids}$$

$$Fe^{3+}\text{on the non-reactive surface of } Al_2O_3 + H_2O_2 + h\nu \rightarrow Fe^{2+} + {}^{\bullet}OH_2 + H^{+}$$

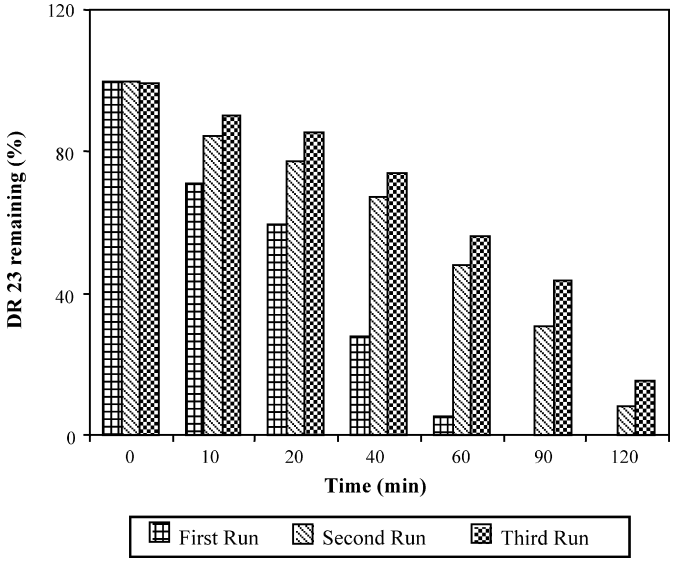

Fig. 12. Catalyst efficiency at different runs: [DR 23] = 5×10^{-4} M, catalyst suspended = 1 g L^{-1}, H_2O_2 = 10 mmol L^{-1}, airflow rate = 8.1 mL s^{-1}, pH = 3 ± 0.1, and $I_0 = 1.381 \times 10^{-6}$ einstein L^{-1} s^{-1}.

Table 2
Comparison of photo-Fenton degradation of DR 23 and RO 4 under optimum conditions for 20 min irradiation.

Dye (5×10^{-4} M)	Decolourisation (%)	Degradation (%)
DR 23[a]	86.95	72.99
RO 4[b]	67.23	54.84

Catalyst suspended = 1 g L^{-1}, airflow rate = 8.1 mL s^{-1}, and $I_0 = 1.381 \times 10^{-6}$ einstein L^{-1} s^{-1}.
[a] pH = 2 ± 0.1, Fe^{2+} = 25%, and H_2O_2 = 10 mmol L^{-1}.
[b] pH = 3 ± 0.1, Fe^{2+} = 15%, and H_2O_2 = 15 mmol L^{-1}.

Fe^{3+}on the non-reactive surface of Al_2O_3+H_2O+$h\nu$

$\rightarrow Fe^{2+}$+•OH+H^+

Initially Fe^{2+} on Al_2O_3 reacts with H_2O_2 producing hydroxyl radicals. The OH radicals attack dye, giving rise to reaction intermediates. Finally, the reaction intermediates are mineralised into CO_2 and H_2O. Fe^{3+} formed on the reactive surface reacts with H_2O_2 or H_2O regenerating Fe^{2+} and •OH_2 or •OH radicals. Hence the reaction is continuous.

3.9. Comparison of photo-Fenton degradation of DR 23 and RO 4

A complete degradation of DR 23 occurs in 60 min where as RO 4 takes 90 min for complete removal under optimum conditions. The results of decolourisation and degradation of 5×10^{-4} mol L^{-1} of DR 23 and RO 4 by Fe^{2+}-Al_2O_3 catalyst under optimum conditions at the time of 20 min irradiation are given in Table 2. The decolourisation and degradation with Fe^{2+}-Al_2O_3 catalyst is more efficient in DR 23 than RO 4. These results indicated that DR 23 could be easily degraded when compared to RO 4. This is due to the difference in the structure of these dyes. RO 4 has a more stable triazine ring and so the degradation efficiency is less in RO 4.

4. Conclusions

The present investigation illustrates that the ferrous sulfate loaded in non-reactive surface of neutral Al_2O_3 is efficient in the degradation of DR 23 and RO 4 in the presence of H_2O_2 and UV light. 25% of Fe(II)-Al_2O_3 and 15% Fe(II)-Al_2O_3 are found to be highly photoactive in the degradation of DR 23 and RO 4 respectively. The other optimum conditions for higher efficiency are: (i) pH 2 for DR 23 and 3 for RO 4, (ii) H_2O_2 concentration—10 mmol L^{-1} for DR 23 and 15 mmol L^{-1} for RO 4. The degradation increases with increase in UV power and decreases with the increase in dye concentration. The catalyst is reusable but the efficiency of the used catalyst is less than the fresh catalyst. The decrease in efficiency of the used catalyst is due to leaching Fe ion from the catalyst. Based on the results, a mechanism has been proposed. Fe(II)-Al_2O_3 catalyst is found to be a viable and reusable catalyst for the treatment of dye wastewater.

Acknowledgements

One of the authors, K. Selvam is thankful to CSIR, New Delhi, for the award of Senior Research Fellowship. We thank Catalysis Laboratory, IIT Madras, Chennai for BET measurements.

References

[1] H.J.H. Fenton, Oxidation of tartaric acid in presence of iron, J. Chem. Soc. 6 (1894) 899.
[2] M.R. Hoffmann, M. Martin, W. Choi, D. Bahnemann, Environmental applications of semiconductor photocatalysis, Chem. Rev. 95 (1995) 69.
[3] J. Kiwi, C. Pulgarin, P. Peringer, Effect of Fenton and photo-Fenton reactions on the degradation of biodegradability of 2-nitrophenols and 4-nitrophenols in water treatment, Appl. Catal. B: Environ. 3 (1994) 335.
[4] A. Safarzadeh Amiri, J.R. Bolton, S.R. Cater, Ferrioxalate-mediated photodegradation of organic pollutants in contaminated water, Water Res. 31 (1997)787.
[5] N.H. Ince, G. Tezcanli, Treatability of textile dye-bath effluents by advanced oxidation: preparation for reuse, Water Sci. Technol. 40 (1999) 183.
[6] M. Muruganandham, M. Swaminathan, Decolourisation of RO 4 by Fenton and photo-Fenton oxidation technology, Dyes Pigments 63 (2004) 315.
[7] M.S. Lucas, J.A. Peres, Decolourisation of the azo dye Reactive black 5 by Fenton and photo Fenton oxidation, Dyes Pigments 71 (2006) 236–244.
[8] Y. Zuo, J. Höigne, Formation of hydrogen peroxide and depletion of oxalic acid in atmospheric water by photolysis of iron(III)-oxalato complexes, Environ. Sci. Technol. 26 (1992) 1014.
[9] J.J. Pignatello, D. Liu, P. Huston, Evidence for an additional oxidant in the photoassisted Fenton reaction, Environ. Sci. Technol. 33 (1999) 1832.
[10] K. Selvam, M. Muruganandham, M. Swaminathan, Enhanced heterogeneous ferrioxalate photo-Fenton degradation of Reactive Orange 4 by solar light, Sol. Energy Mater. Sol. Cells 89 (2005) 61.
[11] S.H. Bossmann, E. Oliveros, S. Göb, S. Siegwart, E.P. Dahlen, L.M. Payawan Jr., M. Straub, M. Wörner, A.M. Braun, New evidence against hydroxyl radicals as reactive intermediates in the thermal and photochemically enhanced Fenton reactions, J. Phys. Chem. A 102 (1998) 5542.
[12] M. Muruganandhan, K. Selvam, M. Swaminathan, A comparative study of quantum yield and electrical energy per order [E_{E0}] for advanced oxidative decolourisation of Reactive azo dyes by UV light, J. Hazard. Mater. 144 (2007) 316.
[13] J. Fernandez, J. Bandara, A. Lopez, Ph. Buffat, J. Kiwi, Photoassisted Fenton degradation of nonbiodegradable azo dye (Orange II) in Fe-free solutions mediated by cation transfer membranes, Langmuir 15 (1999) 185.
[14] I. Muthuvel, M. Swaminathan, Photoassisted Fenton mineralization of Acid Violet 7 by heterogeneous Fe(III)-Al_2O_3 catalyst, Catal. Commun. 8 (2007)981.
[15] J. Fernandez, M.R. Dhananjeyan, J. Kiwi, Evidence for Fenton photoassisted processes mediated by encapsulated Fe ions at biocompatible pH values, J. Phys. Chem. B 104 (2000) 5298.
[16] F. Martinez, G. Calleja, J.A. Melero, R. Molina, Heterogeneous photo-Fenton degradation of phenolic aqueous solutions over iron-containing SBA-15 catalyst, Appl. Catal. B: Environ. 60 (2005) 181.
[17] J. Feng, X. Hu, P. Yue, H. Zhu, G. Lu, Degradation of azo-dye Orange II by a photoassisted Fenton reaction using a novel composite of iron oxide and silicate nanoparticles as a catalyst, Ind. Eng. Chem. Res. 42 (2003) 2058.
[18] W. Ma, Y. Huang, J. Li, M. Cheng, W. Song, J. Zhao, An efficient approach for the photodegradation of organic pollutants by immobilized iron ions at neutral pHs, Chem. Commun. (2003) 1582.
[19] N. Sobana, M. Swaminathan, Nano-Ag particles doped TiO_2 for efficient photodegradation of Direct azo dyes, J. Mol. Catal. 258 (2006) 124.
[20] N. Sobana, M. Swaminathan, Combination effect of ZnO and activated carbon for solar assisted photocatalytic degradation of Direct Blue 53, Sol. Energy Mater. Sol. Cells 91 (2007) 727.
[21] I. Muthuvel, M. Swaminathan, Highly solar active Fe(III) immobilised alumina for the degradation of Acid Violet 7, Sol. Energy Mater. Sol. Cells 92 (2007)857.
[22] H.J. Kuhn, S.E. Braslavsky, R. Schmidt, Chemical actinometry (IUPAC technical report), Pure Appl. Chem. 76 (2004) 2105.
[23] D. Sarkar, D. Mohapatra, S. Ray, S. Bhattacharyya, S. Adak, N. Mitra, Synthesis and characterization of sol–gel derived ZrO_2 doped Al_2O_3 nanopowder, Ceram. Int. 33 (2007) 1275.